

# Teleoperation of a Compliant Avian-Inspired Robot Claw with Continuum Digits

John Mohrmann\*, Jack Schuver\*, Miao Yu, Ian Walker, and Ge Lv

**Abstract**—This paper explores the development of a bio-inspired, large-scale compliant CLAW with continuum digits designed for grasping of delicate objects via human teleoperation. Drawing inspiration from avian perching behaviors, the proposed CLAW utilizes minimal sensing, with input provided through a flexible glove equipped with a single bending sensor, while its shape is controlled via an inertial measurement unit mounted on one of its continuum digits. Unlike previous bird-inspired grippers focused on small-scale perching applications, our approach targets the grasping of delicate objects, addressing challenges associated with the compliance and shape-sensing of soft robotic components. The experiments demonstrate the CLAW’s ability to effectively grasp a variety of objects, as well as proof-of-concept results on “rescuing” objects from a confined environment, showcasing the potential of continuum robots for adaptive manipulation with minimal sensor input. These preliminary results underscore the potential of the proposed continuum-based grippers for applications involving human teleoperators in human-robot collaborative tasks.

## I. INTRODUCTION

Grasping and manipulation are core elements in robotics, and development of robot hands and grippers has been an active area of investigation for many years [1]. Extensive reviews of the literature on robot hands have been presented in [2], [3]. More recently, there has been significant interest in the development of soft hands and grippers, *e.g.*, [4]–[8]. The review paper [9] provides a review of soft robotic hands, highlighting their potential for adaptive and gentle grasping.

Continuum robots, characterized by their smooth, compliant backbones, offer a promising design approach for soft, adaptive robot hands and grippers. Unlike traditional rigid-link robots, they can conform to various shapes upon contact, making them well-suited for grasping and maneuvering in confined environments. Their compliance also enhances safety in human interaction. Over the past two decades, researchers have developed practical continuum robot hardware [10], [11] alongside theoretical and algorithmic advancements [12], leading to successful applications in medical procedures [13], [14]. Despite these advances, continuum robots have seen

This work was supported by the National Science Foundation under Awards 2221126, 2312423, and 2340261. The content is solely the responsibility of the authors and does not necessarily represent the official views of the National Science Foundation.

\* both authors contributed equally to the paper.

J. Mohrmann and J. Schuver are with the Department of Electrical & Computer Engineering, Clemson University, Clemson, SC 29634, USA. {jmohrma, jschuve}@clemson.edu. M. Yu and G. Lv are with the Departments of Mechanical Engineering, Clemson University, Clemson, SC 29634, USA. {myu2, glv}@clemson.edu

I. Walker is with the Department of Electrical Engineering & Computer Science, University of Wyoming, Laramie, WY 82071, USA. iwalker2@uwyo.edu

limited adoption outside the medical field. A comprehensive review of their current state is provided in [15], with studies on their grasping capabilities presented in [16]–[18].

Among various design approaches, one particularly promising strategy is the use of compliant grippers with continuum digits. In this work, we explore the operation of such a gripper inspired by the feet of birds [19], as shown in Fig. 1. Previous studies have proposed bird-inspired robotic hands [20], [21], and bird perching behaviors has influenced the development of manipulators, particularly for drones [22]–[26]. These efforts have primarily focused on small, lightweight continuum digits for grasping solid surfaces. In contrast, this paper investigates a novel approach to grasping delicate objects using an unusually large gripper with continuum digits. One issue with grasping using soft and continuum components is that of identifying and deploying suitable and sufficient sensors. The compliance in soft gripper elements - inherently desirable to support adaptive grasping - makes accurate sensing of their shape challenging.

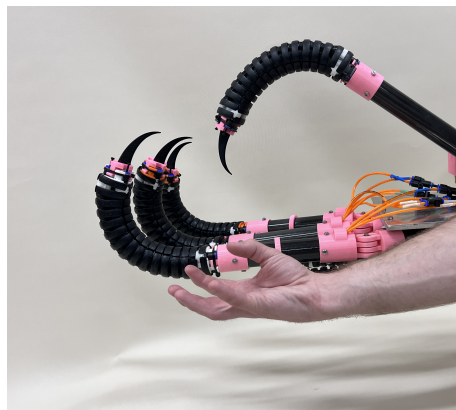


Fig. 1. Continuum robot based, avian-inspired CLAW.

In addition to the limitation in sensing, existing continuum robots often operate on their own, with minimal or even no human interaction. This lack of integration with human users restricts their applicability in tasks requiring real-time adaptation and intuitive control (*e.g.*, a rescue task in a confined environment). Unlike rigid robotic systems, which benefit from well-established teleoperation and haptic feedback methods, continuum robots pose unique challenges due to their high compliance, nonlinear behavior, and infinite degrees of freedom (DoFs) [27]. A largely open issue is the development of effective interaction modalities for human users of soft robots. Traditional control methods, such as joystick or teach-and-repeat approaches, may not fully leverage the

adaptability of continuum structures [28]. More advanced strategies, including haptic feedback, vision-based intent recognition, and learning-based interfaces, could enhance usability and precision [29]. Further research is needed to explore how humans can intuitively guide continuum robots, whether through direct manipulation, wearable interfaces, or multimodal input systems [30]. Addressing these challenges will be crucial for expanding the practical deployment of continuum robots in areas such as assistive robotics and collaborative manipulation.

In this paper, we present the teleoperation of a large-scale compliant robotic CLAW with minimal sensing. The gripper is controlled via an operator using a flexible glove equipped with a single bending sensor, while its shape is regulated based on input from a single inertial measurement unit (IMU) mounted at the proximal end of one of its four compliant continuum digits. The objective is to demonstrate adaptive manipulation capabilities using a minimal sensor set. We map the real-time trajectory of a human operator’s hand to a series of set points based on the constant curvature model, and a Proportional-Integral-Derivative (PID) controller was employed to regulate the CLAW’s motion. Preliminary experimental results involving the grasping of delicate objects and “rescuing” objects from a confined environment validate the effectiveness of this approach.

## II. DEVELOPMENT OF HAND GLOVE SYSTEM

In this section, we present the development of the glove system that can measure the bending angle of human hand when performing a grasping task.

### A. Mechanical Design

We utilized an off-the-shelf glove (Model HyFlex, Ansell, NJ, USA) integrated with a flex sensor resistor to capture the grasping motion of human hands, which will be used as a reference to control the continuum robot based, avian-inspired CLAW (to be introduced in Sec. III). Bending angle of human hands could be challenging to measure given three separate flexing points of each finger. We chose the third proximal inter-phalangeal joint as the primary center of the rotation, as focusing on a single joint lowers computation and system complexity.

Upon flexing of the hand, the distance between the tip of the finger and metacarpophalangeal joint increases. We therefore 3D-printed an anchor and a slide (both glued to the glove) to allow the resistor to move up the knuckle and maintain its rotational center around the proximal inter-phalangeal joint. The 3D-printed anchor and slide assembly consist of 4 components: 1) an anchor located at the center of the back of the hand; 2) a spring that connects the anchor to the slide for returning the flex resistor to its resting position upon relaxation of the hand; 3) a track located just below the metacarpophalangeal joint of the hand; and 4) a slide that rides up and down the track, with its upper limit set by a raised edge stop.

The chosen flex sensor resistor (to be specified in Sec. II-B) is affixed to the slide using adhesives, chosen in part due

to its insulation properties to shield the exposed leads from interference or shorting.

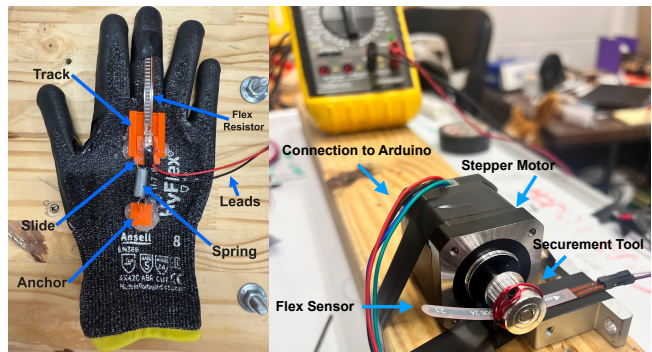


Fig. 2. The glove with the track, slide, spring, and the flex sensor (left), and the testing station with the stepper motor and the securement tool (right).

### B. Electrical System Design

The development of the glove’s electrical system went through two distinct phases. The first phase used an Arduino UNO R3 with an ohmmeter circuit integrated onto a shield, with the SEN 10264 Flex Resistor being the sensor. The ohmmeter circuit used a 55 k $\Omega$  as the reference and the flex resistor as the unknown, where the resistance of the flex sensor was calculated as

$$R_{\text{flex}} = \left( \frac{1024}{V_{\text{raw}}} - 1 \right) \cdot 55\text{k}\Omega. \quad (1)$$

In (1),  $V_{\text{raw}}$  is the raw voltage from the flex sensor resistor, and  $R_{\text{flex}}$  is the calculated sensor resistance. The Arduino UNO R3 received voltage from the ohmmeter circuit and then determined the position of the hand through converting the voltage to resistance, and obtaining the associated bend angle using the model found during calibration.

The flex resistor was calibrated before and after the integration into the ohmmeter, but only post-integration results were used in the integration of the glove into the overall system. We developed a testing platform, which consists of a stepper motor, its driver, a securement tool, and an Arduino UNO board to repeatedly obtain the resistance value with the same bending angles during calibration. The stepper motor was controlled to rotate 24 steps per degree, allowing the securement tool attached to the end of the axle to rotate an expected distance on command. The Arduino was programmed to begin at 0 $^\circ$ , and upon execution, rotate in 9 $^\circ$  steps upon subsequent commands. The flex resistor was attached to the base and securement tool, pulling forward and around the tool when the stepper motor was activated. This allowed the flex resistor to move to the desired angle while maintaining its included radius. A multimeter was connected to the resistor’s leads to measure resistance at each state. A protractor was used to verify the bending angle by measuring from the base to the tip of the rotated resistor section. Overall, we ran the calibration 8 times and then averaged the results.

### C. System Integration

To facilitate communication between the glove and the central controller (*i.e.*, a Raspberry Pi 4B), we took the output

of the ohmmeter and sent it to an analog-to-digital converter (ADC) and then relays the angles to a PID controller for controlling the CLAW. The calibrated values were used to encapsulate the range and magnitude of response from the system, without the need to directly compute the resistance upon actuation. Capacitors are used to filter noises to provide better feedback signals for control.

### III. DEVELOPMENT OF BIO-INSPIRED CLAW

The CLAW's design is derived from avian physiology, specifically that of the anisodactyl and raptorial morphotypes, persisting of three forward facing digits and one rear facing digit as shown in Fig. 3. The CLAW mimics the functionality of these digits on a large scale, containing rigid and continuum segments that function together to be pneumatically actuated in two DoFs: abduction/adduction and extension/flexion.

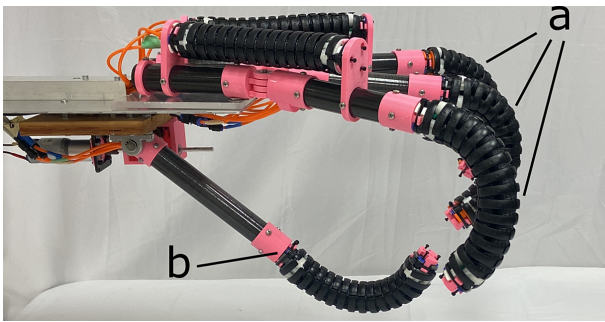


Fig. 3. The CLAW consists of three forward-facing digits (a) and a single rear facing digit (b). The rear facing digit (b) can be actuated at the end of the proximal rigid element by a motor. Figure reproduced from [19]

Each forward facing appendage consists of a proximal continuum section, two rigid bones, a passive revolute joint, and a distal continuum section (Fig. 4). The proximal continuum sections control the adduction/abduction movements of the CLAW, while the distal continuum sections control the extension/flexion movements that are used for grasping. The bones and revolute joint provide mechanical support and strength for the compliant continuum sections. The rear facing appendage consists of a distal continuum section, rigid bone, and a servo driven worm-gear. The combination of the servo and distal muscle allow full movement of the continuum section across a range of positions, permitting gripping of objects varying in size along the flexion/extension DoF.

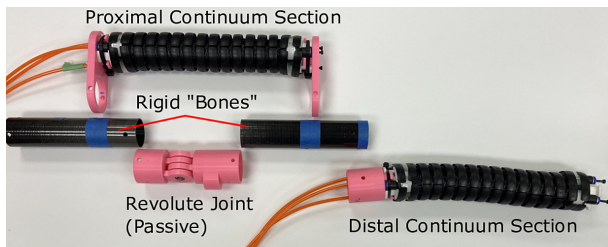


Fig. 4. Assembly of elements for a single outer CLAW digit. Note the rear facing digit include neither the proximal continuum section nor the revolute joint. Figure reproduced from [19].

Each continuum section consists of three extending McKibben muscles that are pneumatically actuated by eight

pressure regulators. The forward facing digit's muscles are divided into groups based on the action they control, *i.e.*, adduction/abduction and extension/flexion, where each DoF is controlled by an independent pressure regulator. Three pressure regulators independently control the reverse-facing appendage, one per muscle in the continuum section. We control these pressure regulators via an Arduino Mega 2560, which amplifies a 0-5V signal into an amplified AC signal. More details about the CLAW's design can be found in [19].

### IV. CONTROL SYSTEM DEVELOPMENT

In this section, we proposed the derivation of the target positions for the CLAW to track based on the constant curvature model, and the PID controller and its integration with the overall glove-CLAW system.

#### A. Constant Curvature Model

Previous experiments and studies [31]–[34] indicate that using Cartesian angle measurements to define the motion of a continuum robot, *e.g.*, CLAW's appendages, results in nonlinear dynamics. Since the CLAW's motion is directly controlled by pneumatic pressure applied to its appendage, we wish to establish a relationship between the input trajectories from the glove and the bending angle of the CLAW. By defining the input trajectories as curvatures rather than a sequence of angles, a linear relationship can be created to approximate segments of a continuum robot. The basis for this model is derived based on the conventional constant curvature model [32]:

$$K = \frac{\theta}{S}, \quad (2)$$

where  $\theta$  is the bending angle,  $S$  is the corresponding arc length, and  $K$  is the curvature. The CLAW appendages bend uniformly, allowing them to be modeled as a single segment, with motion defined by a single curvature set point. This establishes a linear relationship between the CLAW's output angle and the constant curvature model. This relationship can be obtained from simple, measurable properties of the CLAW at the maximum bending angle  $180^\circ$  (through manual bending):

$$K_{\text{Appen},180^\circ} = \frac{\pi}{S_{\text{Appen}}}, \quad (3)$$

where  $K_{\text{Appen},180^\circ}$  and  $S_{\text{Appen}}$  are the curvature and arc length at  $180^\circ$  bending, respectively. We can then leverage (3) to obtain the set point for the CLAW to follow in terms of  $K_{\text{Appen},180^\circ}$  as

$$\theta_{\text{Setpoint}} = \left( \frac{\theta_{\text{IMU}}}{K_{\text{Appen},180^\circ}} \right) K_{\text{Setpoint}} + \theta_0, \quad (4)$$

where  $\theta_{\text{Setpoint}}$  is the target position for the CLAW to follow,  $\theta_{\text{IMU}}$  is the measured angle from an IMU (NGIMU, x-io Technologies Limited, Bristol, UK) mounted to the knuckle of the appendages (Fig. 5),  $K_{\text{Setpoint}}$  is the curvature of the reference position profile (to be defined in Sec. IV-B), and  $\theta_0$  is the initial resting angle of the CLAW. From (4), the CLAW is expected to achieve a linear response based on the targeting curvature and feedback from the NGIMU sensor.

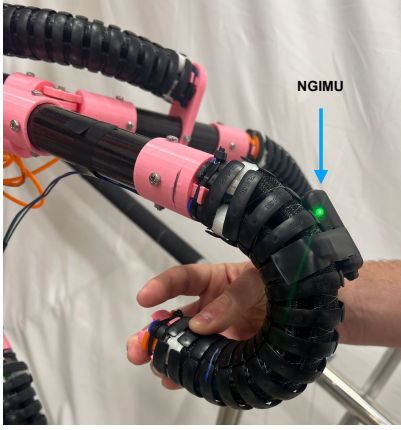


Fig. 5. The CLAW with the NGIMU mounted on the knuckle.

### B. Controller Development

To realize tracking of the hand trajectory in real-time, we employed a PID controller that receives the reference signal from the glove and angular position feedback of the CLAW from the IMU, and produces the control signal (in voltage) to regulate the position of appendages of the CLAW, *i.e.*,

$$u = K_p \cdot e + K_I \cdot \int edt + K_D \cdot \dot{e}, \quad (5)$$

where  $K_p$ ,  $K_I$ , and  $K_D$  are the gains of the PID controller, and error term is defined as  $e := \theta_{\text{Setpoint}} - \theta_{\text{IMU}}$ . To obtain the value of  $\theta_{\text{Setpoint}}$  in real-time, we converted the voltage taken from the glove to a curvature  $K_{\text{Setpoint}}$  and then followed the calculation in (4). Given the voltage and resistance of the glove ohmmeter follow an approximate linear relationship, we calculate  $K_{\text{Setpoint}}$  as

$$K_{\text{Setpoint}} = K_{C_{\text{max}}} - \left( \frac{K_{C_{\text{min}}} - K_{C_{\text{max}}}}{V_{G_{\text{max}}} - V_{G_{\text{min}}}} \right) V_{\text{ADC}}, \quad (6)$$

$$K_{C_{\text{max}}} = \left( \frac{K_{\text{Appen},180^\circ}}{\theta_{\text{IMU}}} \right) \theta_0,$$

$$K_{C_{\text{min}}} = \left( \frac{K_{\text{Appen},180^\circ}}{\theta_{\text{IMU}}} \right) \theta_{\text{IMU,Full}},$$

where  $K_{C_{\text{min}}}$  and  $K_{C_{\text{max}}}$  are the minimum and maximum curvature values exhibited by the CLAW,  $V_{G_{\text{min}}}$  and  $V_{G_{\text{max}}}$  are the minimum and maximum values of the glove voltage  $V_{\text{ADC}}$ , and  $\theta_{\text{IMU,Full}}$  is the maximum possible bending angle of the CLAW when actuated for grasping.

### C. Control System Integration

We used a Raspberry Pi 4 as the central controller for receiving feedback signals from the glove, real-time sensory feedback from the IMU sensor (through UART protocol), and computing the control law  $u$  in (5). An ADS1115 ADC was utilized to facilitate the voltage transfer from the glove to the Raspberry Pi. By reading of voltage from the glove, the ADC was able to provide a continuous voltage range from 1.7–3.1V. The calculated control command is passed to the CLAW through a MCP4728 Digital-to-Analog Converter (DAC) to translate the digital positional voltage to an analog signal. This voltage value is then written to a specific channel

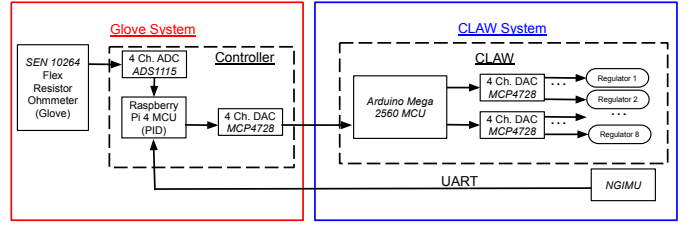


Fig. 6. Overall schematic diagram of the glove-CLAW system.

of the DAC, split into two 8-bit integers for memory purposes, and returned to the CLAW as a 0-5V AC control signal. The overall schematic diagram of the system is given in Fig. 6.

## V. EXPERIMENTAL RESULTS AND DISCUSSION

In this section, we present the proof-of-concept experimental results of the CLAW grasping various objects, as well as performing “rescuing” tasks in two confined environments, both following the grasping motion of human hands. All experimental videos can be viewed here on YouTube.

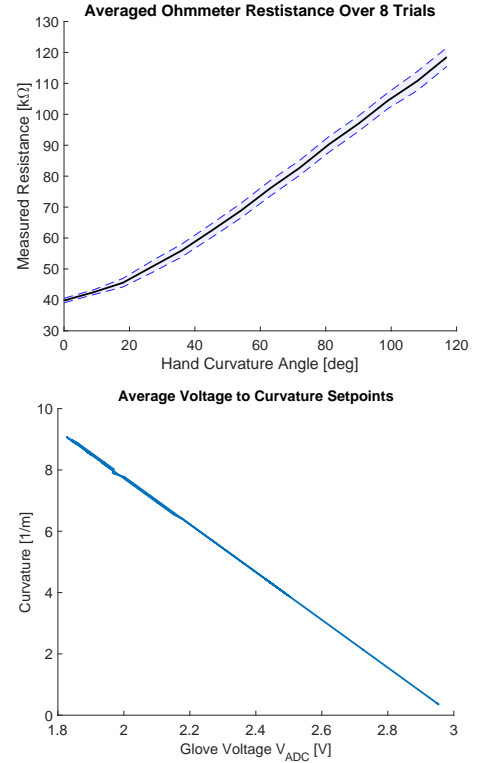


Fig. 7. Mean and  $\pm 1 \cdot$  standard deviation of the flex sensor’s resistance over various hand bending angles (top) and mean value of  $K_{\text{Setpoint}}$  over glove voltage  $V_{\text{ADC}}$  (bottom) across 8 trials.

### A. Verification of Linear Relationship

Before conducting grasping experiments, we first calibrated and flex sensor resistor to verify the assumption that its voltage and the associated bending angle can be described using a linear relationship. We ran the bending test across multiple angular positions for a total of eight trials using the testing platform in Fig. 2 (right), where the results are given in Fig. 7. It is obvious that the relationship between



Fig. 8. The CLAW grasping the balloon, packing sheet, and a piece of foam following the operator’s hand motion.

the sensor’s resistance and the associated bending angle is linear, except with some minor nonlinearity at smaller bending angles. Similarly, Fig. 7 (bottom) shows the linear relationship between the glove voltage  $V_{ADC}$  and the reference curvature  $K_{Setpoint}$ . Given results from Fig. 7, the overall relationship from the hand position to the flex sensor’s resistance/voltage, and then to the curvature value  $K_{Setpoint}$  is linear, justifying the use of (4) for control purposes.

### B. Static Grasping Tasks

We stabilized the CLAW to a fixed structure and employed it to grasp various irregularly shaped objects, including a balloon, a bundle of packing sheet, and a foam packing insert (Fig. 8), all following the motion of a human operator’s hand. Each of these experiments shows the unique versatility of the CLAW’s grasping abilities. The associated PID control signals of one successful grasp (defined as starting with all fingers extended and ended with a fist posture) are demonstrated in Figs. 9. We adjusted the PID control gains through trial-and-error to achieve satisfactory performance, where the fine-tuned gains were given as  $K_p = 0.15$ ,  $K_I = 0.001$ , and  $K_D = 0.03$ . These parameters were then kept as constants throughout the experiments. In all scenarios, the CLAW was able to successfully grasp the objects utilizing the unique characteristics of each of the continuum appendages, without causing any damage to the grasped object.

### C. Rescue Grasping Tasks

The rescue tasks consist of two parts: We then mounted the CLAW to a mobile platform that can move horizontally and performed “rescue” tasks, where the CLAW moved under a bedsheet (rescue task 1, Fig. 10) or opened a cardboard door (rescue task 2, Fig. 11), searched for a plush animal, and pulled it out to safety following the human operator’s hand motions. These two tests were conducted to resemble rescuing tasks in confined environments. For both rescue tasks, cameras were attached to the CLAW to capture and display the first-person perspective during the experiments. We performed task 1 and 2 five and three times respectively to demonstrate the versatility of the CLAW in irregular spaces. Throughout the experiments, we recorded the feedback from the IMU and the set point from the glove, where the averaged results across 5 trials for rescue task 1 are shown in Fig. 12. Overall, the differences are acceptable, indicating the feasibility of the proposed control approach.

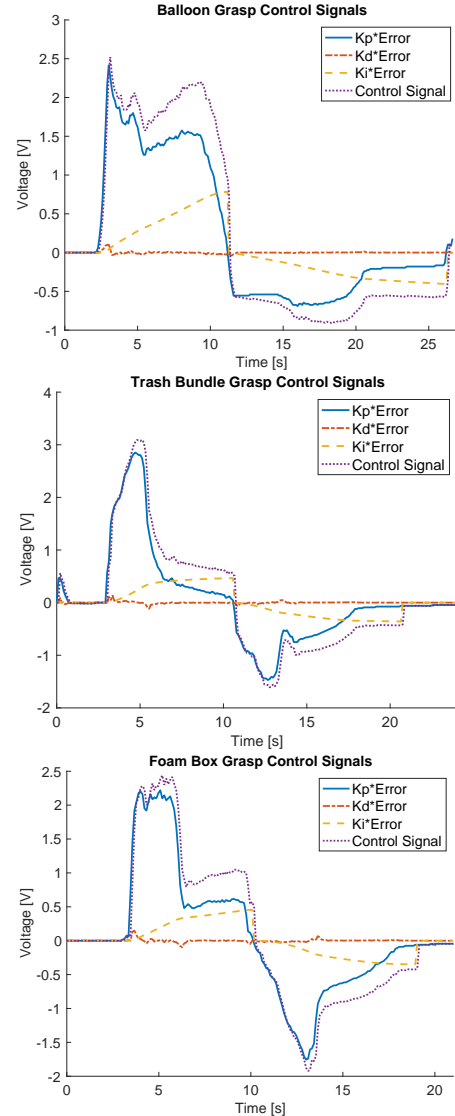


Fig. 9. Control law  $u$  of one successful grasp for the balloon (top), packing sheet (middle), and the foam (bottom).

### D. Constant Curvature Model Performance

Throughout the experiments, we derived the target position  $\theta_{Setpoint}$  based on the assumption that the CLAW’s motion can be described by a constant curvature model. We therefore verified this assumption through plotting the CLAW’s curvature with the measured IMU angle in Fig. 13. The results show a well-defined linear region where the model accurately



Fig. 10. Screenshots of the CLAW performing the rescue task 1, where it crawls underneath the bedsheet via the mobile platform (1), located and grasped the plush animal (2 and 3), and moved it to safety (4). The second row shows the first-person perspective view of the CLAW.

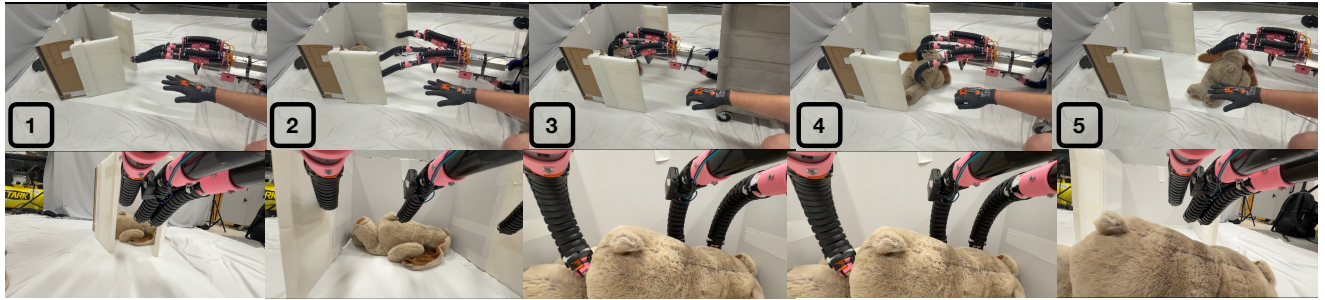


Fig. 11. The CLAW performing the rescue task 2, where it reached the cardboard door (1), opened the door via abduction (2) followed by the hand motion, reached and grasped the plush animal (3 & 4) followed by the hhumanoperator's hand motion, and pulled the animal to safety (5).

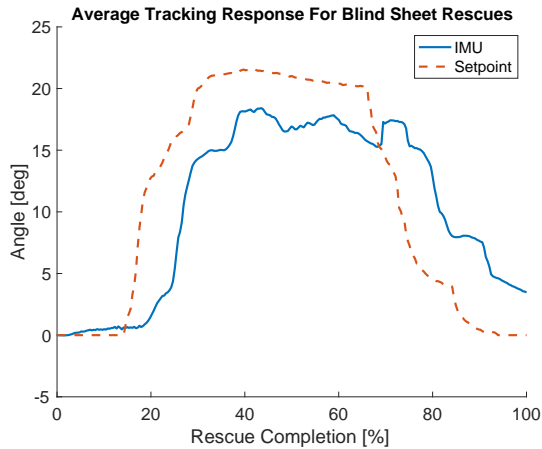


Fig. 12. Mean value of the IMU feedback and the calculated set point for rescue tasks 1 across 5 trials. The results for rescue task 2 are similar thus not demonstrated.

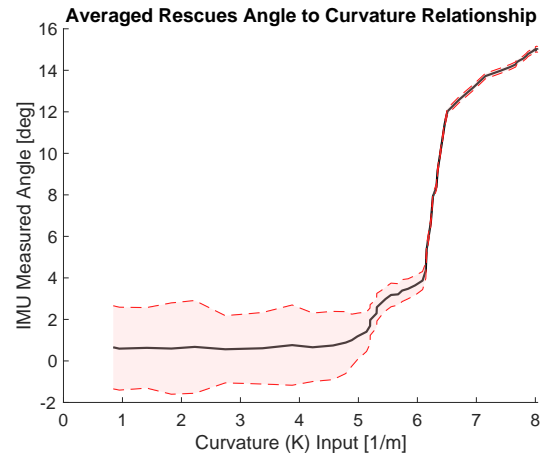


Fig. 13. Mean  $\pm 1$  standard deviation of the measured IMU angle over different values of CLAW over 5 trials in rescue task 1. The linear relationship deteriorates when the CLAW made contact with the plush animal.

represents the system with minimal variance. However, as the curvature input approaches zero, the model's accuracy degrades, leading to increased deviation. Similarly, at higher curvature values, deviations of the linear relationship occur when the CLAW makes contact with the plush animal, though the trend remains largely linear. We will further investigate these nonlinear regions in future studies.

## VI. CONCLUSIONS

In this paper, we proposed the teleoperation of a compliant, avian-inspired robot CLAW with only minimal amount of

sensor. We sampled the operator's hand bending angle via a flexible sensor resistor and mapped it to a series of target set points for the CLAW to track based on the constant curvature model. A PID controller was then employed to facilitate tracking of these set points with the CLAW's bending angle measured through an IMU sensor. We conducted proof-of-concept experiments of the CLAW grasping various delicate objects with various shapes, as well as "rescuing" tasks on a plush animal to grasp and pull it to safety in two confined environments. Despite using only a single

IMU sensor, the CLAW was able to accurately grasp the items without causing any damage. These preliminary results demonstrate the potential of the proposed research in human-robot collaborative applications, such as disaster rescue, repairs in hazardous environments, and handling delicate objects, where adaptive manipulation and shared autonomy are crucial for success. Future study includes investigating other forms of controller for grasping tasks, as well as integrating additional flex sensor resistors on the glove to better capture human operator's hand motion.

#### ACKNOWLEDGEMENT

We thank Nithesh Kumar for his help in the experiments presented in this paper.

#### REFERENCES

- [1] I. Kato, *Mechanical hands Illustrated*. Survey Japan, 1982.
- [2] A. Bicchi, "Hands for dexterous manipulation and robust grasping: A difficult road toward simplicity," *IEEE Transactions on Robotics and Automation*, vol. 16, no. 6, p. 652–662, 2000.
- [3] C. Melchiorri and M. Kaneko, "Robot hands," in *Springer Handbook of Robotics, 2nd Ed., B. Siciliano and O. Khatib, Eds*, vol. Chapter 19, 2016, pp. 463–480.
- [4] K. Galloway, K. Becker, B. Phillips, J. Kirby, S. Licht, D. Tchernov, R. Wood, and D. Gruber, "Soft robotic grippers for biological sampling on deep reefs," *Soft Robotics*, vol. 3, no. 1, pp. 23–33, 2016.
- [5] V. Ho and S. Hirai, "Design and analysis of a soft-fingered hand with contact feedback," *IEEE Robotics and Automation Letters*, vol. 2, no. 2, pp. 491–498, 2017.
- [6] N. Sinatra, C. Teeple, D. Vogt, K. Parker, D. Gruber, and R. Wood, "Ultragentle manipulation of delicate structures using a soft robot gripper," *Science Robotics*, vol. 4, pp. 1–11, 2019.
- [7] Y. Liu, Q. Bi, and Y. Li, "Development of a bio-inspired soft robotic gripper based on tensegrity structures," in *IEEE/RSJ International Conference on Intelligent Robots and Systems (IROS)*, 2021, pp. 7398–7403.
- [8] L. Beddow, H. Wurdemann, and D. Kanoulas, "A caging inspired gripper using flexible fingers and a movable palm," in *IEEE/RSJ International Conference on Intelligent Robots and Systems (IROS)*, 2021, pp. 7195–7200.
- [9] J. Hughes, U. Culha, F. Giardina, F. Guenther, A. Rosendo, and F. Iida, "Soft manipulators and grippers: a review," *Frontiers in Robotics and AI*, vol. 3, p. 69, 2016.
- [10] Y. Kim and J. P. Desai, "Design and kinematic analysis of a neurosurgical spring-based continuum robot using SMA spring actuators," in *IEEE/RSJ International Conference on Intelligent Robots and Systems (IROS)*, 9 2015, pp. 1428–1433.
- [11] P. H. Nguyen, I. B. Mohd, C. Sparks, F. L. Arellano, W. Zhang, and P. Polygerinos, "Fabric soft poly-limbs for physical assistance of daily living tasks," in *Proceedings IEEE International Conference on Robotics and Automation*, 2019, pp. 8429–8435.
- [12] F. Boyer, V. Lebastard, F. Candelier, and F. Renda, "Dynamics of continuum and soft robots: a strain parameterization based approach," *IEEE Transactions on Robotics*, vol. 37, no. 3, pp. 847–863, 2021.
- [13] H. Liu, A. Farvardin, S. A. Pedram, I. Iordachita, R. H. Taylor, and M. Armand, "Large deflection shape sensing of a continuum manipulator for minimally-invasive surgery," in *Proceedings IEEE International Conference on Robotics and Automation*, 2015, pp. 201–206.
- [14] J. Wang, J. Ha, and P. Dupont, "Steering a multi-armed robotic sheath using eccentric precurved tubes," in *Proceedings IEEE International Conference on Robotics and Automation*, 2019, pp. 9834–9840.
- [15] M. Russo, S. Sadati, X. Dong, A. Mohammad, I. Walker, C. Bergeles, X. Xu, and D. Axinte, "Continuum robots: An overview," *Advanced Intelligent Systems*, pp. 1–25, 2023.
- [16] D. Lane, J. Davies, G. Robinson, D. O'Brien, J. Sneddon, E. Seaton, and A. Elfstrom, "The amadeus dextrous subsea hand: Design, modeling, and sensor processing," *IEEE Journal of Oceanic Engineering*, vol. 24, no. 1, pp. 96–111, 1999.
- [17] J. Li and J. Xiao, "Determining "grasping" configurations for a spatial continuum manipulator," in *IEEE/RSJ International Conference on Intelligent Robots and Systems (IROS)*, 2011, pp. 4207–4214.
- [18] J. Li, Z. Teng, J. Xiao, A. Kapadia, A. Bartow, and I. Walker, "Autonomous continuum grasping," in *IEEE/RSJ International Conference on Intelligent Robots and Systems (IROS)*, 2013, pp. 4569–4576.
- [19] M. Stokes, J. Mohrmann, C. Frazelle, I. Walker, and G. Lv, "The claw: An avian-inspired, large scale hybrid rigid-continuum gripper," *Robotics*, vol. 13, no. 52, pp. 1–13, 2024.
- [20] A. Ramos and I. Walker, "Raptors: Inroads into multifingered grasping," in *IEEE/RSJ International Conference on Intelligent Robots and Systems (IROS)*, 1998, pp. 467–475.
- [21] F. Nabi, K. Sundaraj, V. Vijejan, M. Shafiq, R. Planiappan, I. Talib, and H. Rehman, "A novel design of robotic hand based on bird claw model," *Journal of Physics: Conference Series, IOP Publishing.*, vol. 1997, no. 1, p. 012034, 2021.
- [22] S. Backus, L. Odhner, and A. M. Dollar, "Design of hands for aerial manipulation: Actuator number and routing for grasping and perching," in *IEEE/RSJ International Conference on Intelligent Robots and Systems (IROS)*, 2014, p. 40.
- [23] C. Doyle, J. Bird, T. Isom, C. Johnson, J. Kallman, J. Simpson, R. King, J. Abbott, and M. Minor, "Avian-inspired passive perching mechanism for robotic rotorcraft," in *IEEE/RSJ International Conference on Intelligent Robots and Systems (IROS)*, 2011, p. 4975–4980.
- [24] W. Roderick, M. Cutkosky, and D. Lentink, "Bird-inspired dynamic grasping and perching in arboreal environments," *Science Robotics*, vol. 6, no. 61, 2021.
- [25] A. McLaren, Z. Fitzgerald, G. Gao, and M. Liarokapis, "A passive closing, tendon driven, adaptive robot hand for ultra-fast, aerial grasping and perching," in *IEEE International Conference on Intelligent Robots and Systems (IROS)*, 2019, pp. 5602–5607.
- [26] J. Thomas, J. Polin, K. Sreenath, and V. Kumar, "Avian-inspired grasping for quadrotor micro uavs," in *ASME International design engineering technical conferences and computers and information in engineering conference*, 2013, p. V06AT07A014–V06AT07A014.
- [27] C. Della Santina, C. Duriez, and D. Rus, "Model-based control of soft robots: A survey of the state of the art and open challenges," *IEEE Control Systems Magazine*, vol. 43, no. 3, pp. 30–65, 2023.
- [28] C. Laschi, B. Mazzolai, and M. Cianchetti, "Soft robotics: Technologies and systems pushing the boundaries of robot abilities," *Science robotics*, vol. 1, no. 1, p. eaah3690, 2016.
- [29] D. Rus and M. T. Tolley, "Design, fabrication and control of soft robots," *Nature*, vol. 521, no. 7553, pp. 467–475, 2015.
- [30] C. Della Santina, M. Bianchi, G. Grioli, F. Angelini, M. Catalano, M. Garabini, and A. Bicchi, "Controlling soft robots: balancing feedback and feedforward elements," *IEEE Robotics & Automation Magazine*, vol. 24, no. 3, pp. 75–83, 2017.
- [31] R. J. Webster III and B. A. Jones, "Design and kinematic modeling of constant curvature continuum robots: A review," *The International Journal of Robotics Research*, vol. 29, no. 13, pp. 1661–1683, 2010.
- [32] B. A. Jones and I. D. Walker, "Kinematics for multisection continuum robots," *IEEE Transactions on Robotics*, vol. 22, no. 1, pp. 43–55, 2006.
- [33] M. Rolf and J. J. Steil, "Constant curvature continuum kinematics as fast approximate model for the bionic handling assistant," in *2012 IEEE/RSJ International Conference on Intelligent Robots and Systems*. IEEE, 2012, pp. 3440–3446.
- [34] S. Neppalli and B. A. Jones, "Design, construction, and analysis of a continuum robot," in *2007 IEEE/RSJ International Conference on Intelligent Robots and Systems*. IEEE, 2007, pp. 1503–1507.